Journal of Biomedical Optics

BiomedicalOptics.SPIEDigitalLibrary.org

Photoacoustic imaging of carotid artery atherosclerosis

Pieter Kruizinga
Antonius F. W. van der Steen
Nico de Jong
Geert Springeling
Jan Lukas Robertus
Aad van der Lugt
Gijs van Soest

SPIE.

Photoacoustic imaging of carotid artery atherosclerosis

Pieter Kruizinga,[a,*] Antonius F. W. van der Steen,[a,b,c,d] Nico de Jong,[a,b,c] Geert Springeling,[a] Jan Lukas Robertus,[e] Aad van der Lugt,[f] and Gijs van Soest[a]

[a]Erasmus Medical Center, Thorax Center, P.O. Box 2040, 3000 CA Rotterdam, The Netherlands
[b]Delft University of Technology, Faculty Applied Sciences, P.O. Box 5, 2600 AA, Delft, The Netherlands
[c]Interuniversity Cardiology Institute of The Netherlands, P.O. Box 19258, 3501 DG Utrecht, The Netherlands
[d]Chinese Academy of Sciences, Shenzhen Institutes of Advanced Technology, Shenzhen 518055, China
[e]Erasmus Medical Center, Department of Pathology, P.O. Box 2040, 3000 CA Rotterdam, The Netherlands
[f]Erasmus Medical Center, Department of Radiology, P.O. Box 2040, 3000 CA Rotterdam, The Netherlands

Abstract. We introduce a method for photoacoustic imaging of the carotid artery, tailored toward detection of lipid-rich atherosclerotic lesions. A common human carotid artery was obtained at autopsy, embedded in a neck mimicking phantom and imaged with a multimodality imaging system using interstitial illumination. Light was delivered through a 1.25-mm-diameter optical probe that can be placed in the pharynx, allowing the carotid artery to be illuminated from within the body. Ultrasound imaging and photoacoustic signal detection is achieved by an external 8-MHz linear array coupled to an ultrasound imaging system. Spectroscopic analysis of photoacoustic images obtained in the wavelength range from 1130 to 1250 nm revealed plaque-specific lipid accumulation in the collagen structure of the artery wall. These spectroscopic findings were confirmed by histology. [DOI: 10.1117/1.JBO.19.11.110504]

Keywords: photoacoustics; spectroscopy; tissue optics; atherosclerosis.

Paper 140532LR received Aug. 21, 2014; accepted for publication Oct. 22, 2014; published online Nov. 21, 2014.

The carotid artery (CA) supplies the brain with oxygenated blood. A healthy CA consists of elastic collagen-rich material, allowing it to sustain large and rapid variations in blood pressure. A CA affected by atherosclerosis shows degradation of the collagen structure, thickening of the intima, and formation of complex plaques that contain regions with a lipid-rich necrotic core, calcifications, and often intraplaque hemorrhage. Such vulnerable plaques may rupture and cause cerebral ischemic events.[1] The CA is easily accessible for noninvasive imaging, making it a viable target for the screening of a population at risk for cardiovascular or cerebrovascular events.[2] Common imaging modalities used for CA screening are ultrasound (US), x-ray computed tomography (CT), and magnetic resonance imaging. These techniques provide mostly morphological information, such as vessel wall thickening, accumulation of atherosclerosis, and luminal narrowing. They, however, lack the capability of providing chemically specific information crucial in the clinical evaluation of CA.[3] There is an unmet clinical need for a diagnostic technique that can improve risk stratification based on CA plaque characteristics. In the variable composition of atherosclerotic tissue, several plaque lipids have been identified that are associated with vulnerability.[4] Noninvasive imaging of CA plaque lipidomics may better assess the risk of future events to inform medical or surgical therapeutic strategies.

Photoacoustic (PA) spectroscopy is a method to image tissue composition using the chemically specific optical absorption spectrum for contrast. For vulnerable plaque imaging, we aim to visualize plaque lipids. Distinct spectral features in the near-infrared absorption spectrum as sampled by intravascular PA (IVPA) can be exploited to identify lipids[5,6] and to discriminate between fatty acids in normal tissue and cholesterol species found in plaques.[7,8] In this paper, we investigate the possibility of noninvasive PA imaging of CA plaques, with the aim of distinguishing lipid-rich plaque from fibrous tissue and healthy vessel wall.

Conventional PA devices operate in reflection mode, delivering the light close to the US probe.[9] For imaging the CA in patients, this approach meets with several problems. Seen from the skin, the CA is a fairly deep target, overlaid by skin, muscle, and often the jugular vein. Based on CT-angiography data (100 patients) we found an average distance of 2.9 cm from the skin to the common CA, and only 1.2 cm between the pharynx and the CA. The skin is a strongly light attenuating tissue,[10] particularly if there is a layer of subcutaneous fat, which we expect to be common in the patient population to be investigated with this technique. There will be a strong PA signal generated near the surface of the transducer,[11] and incomplete overlap between the noncollinear light and US receiving beams, leading to signal generation outside the imaging plane.[12] We, therefore, propose to image the CA by means of interstitial illumination (from the pharynx) and external (neck side) US detection, aiming to circumvent the aforementioned problems [Fig. 1(a)].

To test whether internal CA illumination can work for PA imaging, we built a small optical probe comprising a multimode silica fiber (400 μm core, low hydroxyl concentration; Pioneer Optics) with a 34 deg angle (yielding maximum light reflection in a 0.22 NA fiber) polished tip covered by a quartz cap deflecting the beam. The fiber was embedded in a 1.25 mm rigid steel tube to allow easy handling for the beam characterization and controlled phantom experiments. A flexible probe for *in vivo* application was also built and tested, but was not used in the experiments described in this paper.

The optical fiber was coupled to a wavelength tunable pulsed laser (OPOTEK Vibrant B/355-II) using a tapered fiber (1 mm entrance, 360 μm exit diameter; Oxford Electronics, Four Marks, UK). The average pulse energy out of the optical probe at 1200 nm was 2.5 mJ in a spot of ~5 mm diameter, which results in a fluence well below the ANSI safety limit of 100 mJ/cm^2. For PA signal acquisition and US imaging, we used a conventional linear US array (ATL 12L5; center frequency 8 MHz, 256 elements) interfaced to a research US system (Verasonics V1; 256 transmit and 128 receive channels).

*Address all correspondence to: Pieter Kruizinga, E-mail: p.kruizinga@erasmusmc.nl

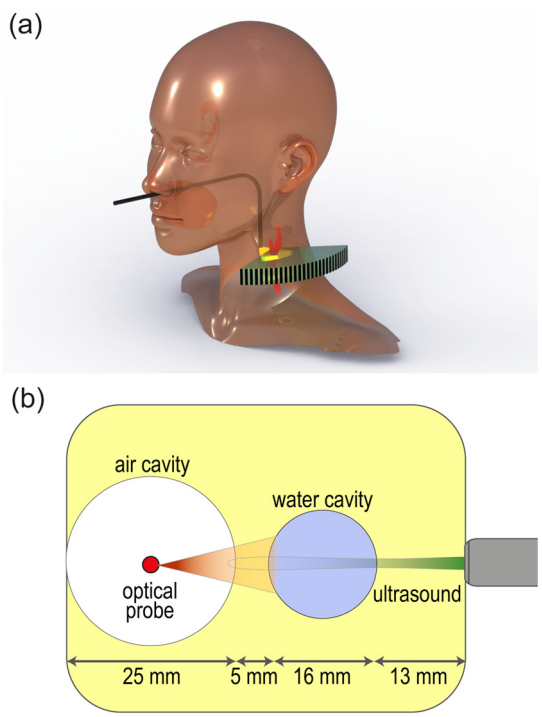

Fig. 1 (a) An impression of the proposed method for photoacoustic imaging of the carotid artery employing internal illumination via the pharynx and external signal detection and ultrasound imaging using a concave array via the neck side. (b) Schematic overview of the neck phantom.

We mimicked the *in vivo* imaging geometry with a phantom made with 18 g agar, 500 ml water, and 1.5 g 5 to 75 μm SiO_2 particles (Sigma-Aldrich).[13] One air-filled cavity (25 mm diameter) in the phantom mimicked the pharynx; another cavity is filled with water to hold the imaging target [see Fig. 1(b)]. The rigid optical probe was mounted on an electronically controllable rotation motor (T-RS60A, Zaber Technologies) and a home-built manual linear stage for vertical positioning. *Ex vivo* validation of the proposed imaging method was performed with a postmortem common carotid artery (CCA) obtained at autopsy from the Department of Pathology of the Erasmus Medical Center (MC), according to a protocol sanctioned by the Medical Ethics Committee of the Erasmus MC. The artery was fixated overnight using 4% buffered formaldehyde to prevent tissue degradation during imaging. The artery was put upright in the phantom cavity filled with a saline solution.

We performed PA spectroscopic imaging of the CCA using 25 wavelengths ranging from 1130 to 1250 nm with steps of 5 nm. The received PA signals were amplified, digitized (14-bits, 45 MHz sampling), and averaged 64 times prior to Fourier domain beamforming.[14] For every scan, we obtained a three-dimensional stack of 25 PA spectral images and one US image. US imaging was performed using a synthetic aperture transmit-receive sequence and dynamic beamforming in receive and image elements. For both PA and US imaging, a middle aperture consisting of 128 elements was used.

We designed a three-step tissue classification method using least-squares spectral unmixing.[15] We first normalize every pixel spectrum $\mathbf{x}_i$ and every reference $\mathbf{x}_R$ to its maximum value. In the second step, we unmix the spectrum at every PA image pixel with four lipid reference spectra,[7] using the lsqnonneg.m MATLAB® routine. Finally, pixels with a high residual (using a heuristically determined threshold of $||\mathbf{x} - \mathbf{x}_R|| > 2$) were further decomposed with two known tissue spectra (water and collagen[16]). The reference spectrum with the largest weight was used to label the main tissue component detected in the image. We omit a compensation for possible coloring of the local fluence as a result of wavelength-dependent light attenuation. Water and collagen, the dominant absorbers in the mucous and muscle tissue occurring in the path from the pharynx to the CA, have relatively weak and slowly varying absorption spectra in the wavelength range from 1130 to 1250 nm, compared to strong and distinct absorption of the lipids we seek to detect. This is sufficient for classification of the most abundant tissue component, unlike quantitative spectroscopy, which retrieves absolute concentrations of chromophores.[17]

In Fig. 2, we show three spectral (1130, 1200, and 1250 nm) PA images superimposed on an US image obtained from the diseased CCA inside the neck phantom. The relatively high water absorption around 1200 nm causes PA signal generation at the pharynx–neck interface (left side). PA signal generation inside the artery wall is observed in all three images with a clear signal increase inside the artery wall at 1200 nm [Fig. 2(c)]. No PA signal was detected for the far wall of the CCA.

Figure 3 shows the US image with the result of the PA spectral unmixing for the tissue types superimposed: water, collagen, fatty acids, and cholesterol species dominant in diseased plaque tissue. The artery generates PA signals that are spectrally distinguishable by their collagen and lipid signature. Inside the artery wall, we observe a lipid accumulation inside the collagen structure. Histology using Oil Red O lipid staining [right images in Figs. 3(b) and 3(c)] confirms the presence of lipids at the location where the PA tissue classification shows plaque lipids. The general morphology highlighted with Resorcine Fuchsine stain [left images in Figs. 3(b) and 3(c)] confirms the presence of a collagen-rich tissue at the location where PA tissue classification shows collagen.

The data shown in Fig. 3 suggest that it is possible to image atherosclerotic plaque composition using spectroscopic PA imaging in the CA. We demonstrated image contrast specific for

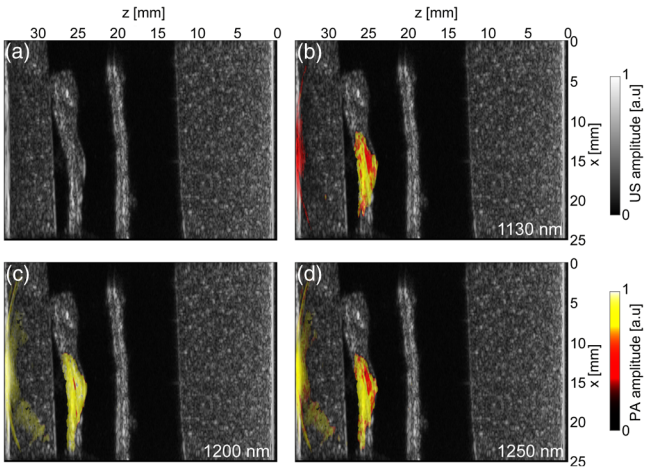

Fig. 2 (a) Ultrasound (US) image of a diseased human carotid artery inside a neck phantom. (b) to (d) Superimposed photoacoustic (PA) images obtained at 1130, 1200, and 1250 nm, respectively. The US transducer was positioned on the right and the light was administered from the probe positioned in the cavity mimicking the pharynx on the left. The US image shows mild thickening of the intima. In the PA images, we observe signals from the artery wall with localized signal increase at 1200 nm (c) indicative of the presence of lipids.

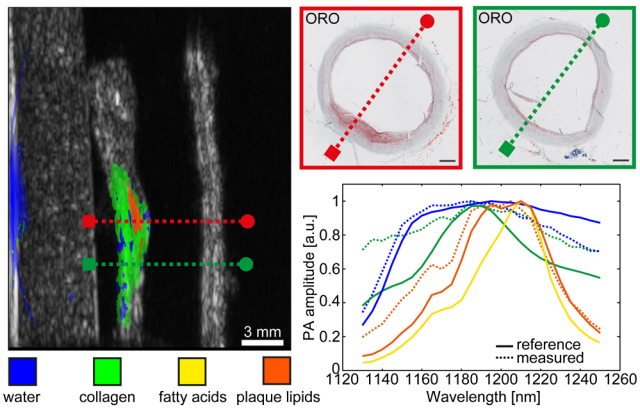

Fig. 3 PA imaging of a lipid plaque in a carotid artery *ex vivo*. Left panel: tissue composition (water, collagen, fatty acids, and plaque lipids) identified by PA spectroscopy are color coded and overlaid on the US image. Plaque lipid accumulation inside the collagen structure of the artery wall can be observed. Top right: histologic sections of two sites in the image using Oil Red O stain indicating the presence of lipid. The dashed lines indicate the corresponding imaging plane. Bottom right: normalized reference and measured spectra used for spectral unmixing.

plaque lipids in an *ex vivo* setting that closely mimics the *in vivo* geometry, exploiting endogenous absorption contrast in the wavelength range from 1130 to 1250 nm. US imaging revealed intima thickening caused by the plaque, but could not provide tissue-specific contrast. Figures 2 and 3 also demonstrate the feasibility of using a transmission geometry for PA carotid imaging, employing internal illumination with a small diameter optical probe and external signal detection.

The data presented here show that it is possible to use near-infrared light near 1.2 μm to image lipids at a relatively large depth, water absorption notwithstanding. The phantom used here does not mimic the complexity of the neck in terms of tissue heterogeneity, optical, and acoustic attenuation. It does represent the relevant scattering and geometrical properties, however, as well as the dominant water absorption. An *in vivo* imaging device would use a flexible optical probe that can be passed through the nose down to the pharynx, comparable to the position of a nasogastric feeding tube. Probe localization and positioning can be aided by real-time monitoring of the PA response of the pharynx wall. The small size of such a probe (~1 mm) means that patient comfort is not compromised. The optical design of the tip is a subject for further study, with the aim to minimize the applied fluence while optimizing the sensitivity and noise characteristics of the US signal detection chain. An improved signal-to-noise ratio would also permit imaging of the entire circumference of the artery [see Figs. 2 and 3]. The use of a customized transducer and optimal signal acquisition, as was demonstrated in Ref. 9, could provide the means to translate this idea to an *in vivo* clinical imaging device. *In vivo* imaging would require further improvements in speed (both the scan speed and pulse rate) of the laser.

In contrast to IVPA, it is quite conceivable to perform multi-wavelength spectroscopic imaging *in vivo*. This opens up the possibility to study patient-specific plaque lipid profiles, which may provide new variables for prognostic imaging of vulnerable plaque. The example included in this study shows that lipids can be detected in a plaque that looks very mild by US, which only shows a geometrical assessment. The data we show in this letter demonstrate that this does not adequately characterize the disease. Likewise, in more advanced plaques, there is a wide variety in lipid composition, and some of these components are associated with plaque instability.[4] With spectroscopic PA imaging, we may noninvasively study plaque lipidomics *in vivo*.

In this study, we introduced a new technique for chemically specific imaging of carotid atherosclerosis. We demonstrated that the CA can be imaged using internal illumination from the pharynx, external signal detection, and external US imaging. We obtained spectral information in the wavelength range from 1130 to 1250 nm to identify plaque-specific lipids. This technique has the potential to provide new information for risk stratification or to reveal early stages of atherosclerosis, as was demonstrated in this letter with a diseased postmortem human CCA.

Acknowledgments

The authors would like to thank Kim Kuijt-van Gaalen for the histology work. The authors also thank Dr. Koen W. A. van Dongen and Dr. Martin D. Verweij for using the Verasonics system, which was funded by ZonMW.

References

1. S. Carr et al., "Atherosclerotic plaque rupture in symptomatic carotid artery stenosis," *J. Vasc. Surg.* **23**(5), 755–766 (1996).
2. P. K. Shah, "Screening asymptomatic subjects for subclinical atherosclerosis: can we, does it matter, and should we?," *J. Am. Coll. Cardiol.* **56**(2), 98–105 (2010).
3. N. Nighoghossian, L. Derex, and P. Douek, "The vulnerable carotid artery plaque: current imaging methods and new perspectives," *Stroke* **36**(12), 2764 (2005).
4. C. Stegemann et al., "Comparative lipidomics profiling of human atherosclerotic plaques," *Circ. Cardiovasc. Genet.* **4**(3), 232–242 (2011).
5. B. Wang et al., "Detection of lipid in atherosclerotic vessels using ultrasound-guided spectroscopic intravascular photoacoustic imaging," *Opt. Express* **18**(5), 4889–4897 (2010).
6. K. Jansen et al., "Intravascular photoacoustic imaging of human coronary atherosclerosis," *Opt. Lett.* **36**(5), 597–599 (2011).
7. K. Jansen et al., "Lipid detection in atherosclerotic human coronaries by spectroscopic intravascular photoacoustic imaging," *Opt. Express* **21**(18), 21472–21484 (2013).
8. K. Jansen et al., "Spectroscopic intravascular photoacoustic imaging of lipids in atherosclerosis," *J. Biomed. Opt.* **19**(2), 026006 (2014).
9. A. Dima and V. Ntziachristos, "Non-invasive carotid imaging using optoacoustic tomography," *Opt. Express* **20**(22), 25044–25057 (2012).
10. A. Bashkatov et al., "Optical properties of human skin, subcutaneous and mucous tissues in the wavelength range from 400 to 2000 nm," *J. Phys. D: Appl. Phys.* **38**(15), 2543 (2005).
11. C. Kim et al., "Deeply penetrating in vivo photoacoustic imaging using a clinical ultrasound array system," *Biomed. Opt. Express* **1**(1), 278–284 (2010).
12. L. G. Montilla et al., "Real-time photoacoustic and ultrasound imaging: a simple solution for clinical ultrasound systems with linear arrays," *Phys. Med. Biol.* **58**(1), N1 (2013).
13. J. Cook, R. Bouchard, and S. Emelianov, "Tissue-mimicking phantoms for photoacoustic and ultrasonic imaging," *Biomed. Opt. Express* **2**(11), 3193–3206 (2011).
14. B. Treeby and B. Cox, "k-wave: Matlab toolbox for the simulation and reconstruction of photoacoustic wave fields," *J. Biomed. Opt.* **15**(2), 021314 (2010).
15. S. Kim et al., "In vivo three-dimensional spectroscopic photoacoustic imaging for monitoring nanoparticle delivery," *Biomed. Opt. Express* **2**(9), 2540–2550 (2011).
16. T. Allen and P. Beard, "Photoacoustic characterisation of vascular tissue at NIR wavelengths," *Proc. SPIE* **7177**, 71770A (2009).
17. B. Cox et al., "Quantitative spectroscopic photoacoustic imaging: a review," *J. Biomed. Opt.* **17**(6), 0612021 (2012).